



Get Clarity On Generics

Cost-Effective CT & MRI Contrast Agents

**FRESENIUS
KABI**

[WATCH VIDEO](#)

AJNR

This information is current as
of August 16, 2025.

Reduced Patient Radiation Exposure during Neurodiagnostic and Interventional X-Ray Angiography with a New Imaging Platform

K. van der Marel, S. Vedantham, I.M.J. van der Bom, M.
Howk, T. Narain, K. Ty, A. Karellas, M.J. Gounis, A.S. Puri
and A.K. Wakhloo

AJNR Am J Neuroradiol 2017, 38 (3) 442-449

doi: <https://doi.org/10.3174/ajnr.A5049>

<http://www.ajnr.org/content/38/3/442>

Reduced Patient Radiation Exposure during Neurodiagnostic and Interventional X-Ray Angiography with a New Imaging Platform

K. van der Marel, S. Vedantham, I.M.J. van der Bom, M. Howk, T. Narain, K. Ty, A. Karellas, M.J. Gounis, A.S. Puri, and A.K. Wakhloo



ABSTRACT

BACKGROUND AND PURPOSE: Advancements in medical device and imaging technology as well as accruing clinical evidence have accelerated the growth of the endovascular treatment of cerebrovascular diseases. However, the augmented role of these procedures raises concerns about the radiation dose to patients and operators. We evaluated patient doses from an x-ray imaging platform with radiation dose-reduction technology, which combined image noise reduction, motion correction, and contrast-dependent temporal averaging with optimized x-ray exposure settings.

MATERIALS AND METHODS: In this single-center, retrospective study, cumulative dose-area product inclusive of fluoroscopy, angiography, and 3D acquisitions for all neurovascular procedures performed during a 2-year period on the dose-reduction platform were compared with a reference platform. Key study features were the following: The neurointerventional radiologist could select the targeted dose reduction for each patient with the dose-reduction platform, and the statistical analyses included patient characteristics and the neurointerventional radiologist as covariates. The analyzed outcome measures were cumulative dose (kerma)-area product, fluoroscopy duration, and administered contrast volume.

RESULTS: A total of 1238 neurointerventional cases were included, of which 914 and 324 were performed on the reference and dose-reduction platforms, respectively. Over all diagnostic and neurointerventional procedures, the cumulative dose-area product was significantly reduced by 53.2% (mean reduction, $160.3 \text{ Gy} \times \text{cm}^2$; $P < .0001$), fluoroscopy duration was marginally significantly increased (mean increase, 5.2 minutes; $P = .0491$), and contrast volume was nonsignificantly increased (mean increase, 15.3 mL; $P = .1616$) with the dose-reduction platform.

CONCLUSIONS: A significant reduction in patient radiation dose is achievable during neurovascular procedures by using dose-reduction technology with a minimal impact on workflow.

ABBREVIATIONS: CBCT = conebeam CT; CP_{KA} = cumulative dose (kerma)-area product; 3DRA = 3D rotational angiography; EAKR = phantom-entrance air kerma rate; IP_{DRT} = imaging platform with dose-reduction technology; IP_{R} = reference imaging platform; $\text{K}_{\text{a,r}}$ = air kerma rate at the fluoroscopic reference point; LAT = lateral plane of the biplane system; P_{KA} = dose (kerma)-area product; RAKR = image-receptor (detector) entrance air kerma rate

The advancement of neurointerventional practice offers increasingly safe and minimally invasive treatment for a variety of neurovascular diseases. In most cases, the benefits of neuroin-

terventional treatment afforded by fluoroscopic image guidance clearly outweigh the associated radiation risks to patients, especially in comparison with invasive surgical alternatives.¹ However, the growing use of diagnostic procedures and complex fluoroscopy-guided interventions² has led to heightened concerns over ionizing radiation exposure to patients and staff.^{3,4}

To address these concerns, a new commercially available angiographic imaging platform has been developed.⁵ Its dose-reduction strategy applies to digital fluoroscopy and digital subtraction angiography, which accounts for approximately 70%–80% of the total patient radiation dose in vascular angiographic proce-

Received July 15, 2016; accepted after revision October 11.


From the Department of Radiology (K.v.d.M., S.V., M.H., T.N., K.T., A.K., M.J.G., A.S.P., A.K.W.), New England Center for Stroke Research, University of Massachusetts Medical School, Worcester, Massachusetts; and Philips Healthcare (I.M.J.v.d.B.), Best, the Netherlands.


This work was supported, in part, by a grant from Philips Healthcare.

K. van der Marel and S. Vedantham contributed equally to this work.

Paper previously presented at: Annual Meeting of the American Society of Neuroradiology and the Foundation of the ASNR Symposium, April 25–30, 2015; Chicago, Illinois; and Annual Meeting of the Society of NeuroInterventional Surgery, July 27–31, 2015; San Francisco, California.

Please address correspondence to Matthew J. Gounis, PhD, Department of Radiology, New England Center for Stroke Research, 55 Lake Ave N, Room SA-107R, Worcester, MA 01655; e-mail: Matthew.Gounis@umassmed.edu; @MattGounis

 Indicates article with supplemental on-line table.

 Indicates article with supplemental on-line photos

<http://dx.doi.org/10.3174/ajnr.A5049>

dures.^{6,7} At the core of the system is an image postprocessing chain intended to yield diagnostic-quality DSA images at a lower radiation dose to the patient.⁷ Key features of this image-processing chain are multiscale implementations of real-time motion correction, image contrast-dependent temporal averaging, and image noise reduction.⁷ Lower dose acquisitions further allow the use of a smaller focal spot size, reducing magnification-dependent focal spot blur.⁷ Additional hardware optimization includes the use of Cu beam filtration, depending on x-ray tube loading and a narrower x-ray pulse width.⁸ Herein, these noise reduction algorithms and optimized exposure settings⁷ will be collectively referred to as “dose-reduction technology,” which is implemented on the dose-reduction x-ray imaging platform (IP_{DRT}).

Procedural dose reductions and the noninferiority of image quality by using IP_{DRT} have been described for iliac^{9,10} and coronary angiography in adults^{8,11-13} and in children.¹³ For neuroangiographic procedures, a randomized, blinded review of consecutive DSA runs with dose-reduction technology targeting one-fourth of the standard radiation dose showed the ability to maintain diagnostic image quality.⁷ A larger European study in 614 patients provided further evidence of significant reductions in total dose-area products of 62% and 65% for diagnostic and interventional procedures, respectively, while not significantly affecting fluoroscopy time, procedure duration, and the number of acquired images.⁵

A unique aspect of this study was that the neurointerventional radiologist with the dose-reduction platform had the flexibility to select, per case and per acquisition, a targeted dose reduction of 0%, 50%, or 75% as preferred, rather than using a protocol with a

prespecified dose-reduction target.⁵ This paradigm was investigated so that any equivocal image finding may be better visualized at different settings. Our study investigated the dose-reduction achieved in cumulative dose (kerma)-area product (CP_{K_A}) by using such a flexible protocol for common interventional treatments and diagnostic examinations based on a retrospective review of all such procedures during a 2-year period in a North American academic practice. In addition, a key feature of this study that distinguishes it from prior studies was the inclusion of the neurointerventional radiologist (operator) and patient-specific factors as covariates in the statistical analyses.

MATERIALS AND METHODS

This study was conducted in adherence to a protocol approved by our institutional review board and in compliance with the Health Insurance Portability and Accountability Act. Our institutional review board waived the requirement for informed consent for this retrospective study.

Included were neurointerventional and diagnostic procedures performed in 2 dedicated neurointerventional radiology suites during a 2-year time period from January 2, 2013, to December 30, 2014. Initially during approximately 1 year (January 2, 2013, to January 21, 2014), both neurointerventional suites (AlluraXper FD20/10 and FD20/20; Philips Healthcare, Best, the Netherlands) were not equipped with dose-reduction technology. In January 2014, dose-reduction technology was installed in 1 system (Allura Clarity FD20/10; Philips Healthcare). All procedures and examinations performed on this system subsequent to the installation of dose-reduction technology are referred to as performed on the IP_{DRT}. The other system (AlluraXper FD20/20) continued to be operated without dose-reduction technology. All procedures and examinations performed on this system and those performed on the FD20/10 system before installation of dose-reduction technology are referred to as performed on the “reference” platform (IP_R). For the FD20/20 system, the small and large focal spot sizes (nominal) were 0.4 and 0.7 mm in both planes. For the FD 20/10 system, which is equipped with a smaller detector in the lateral (LAT) plane, the small and large focal spot sizes (nominal) were 0.4 and 0.7 mm for the anteroposterior plane and 0.5 and 0.8 mm for the lateral plane.

The programmed maximum entrance air kerma rates (EAKRs) for each of the 3 available fluoroscopy modes were reduced for IP_{DRT} compared with IP_R. The frame rate, x-ray beam filtration, and maximum EAKR are summarized in Table 1 and were identical for both planes. For both platforms, fluoroscopic

mode II was the default mode. For this mode, quality-control audits performed by an independent American Board of Radiology–certified diagnostic medical physicist encompassing the study period were collected and were used to validate the system-reported air kerma rate at the fluoroscopic reference point ($\dot{K}_{a,r}$) (Table 2). Because the deviations from unity for the ratios of measured and system-reported $\dot{K}_{a,r}$ were comparable with external dosimeter readings and positioning uncertainties,¹⁴ no correction was performed

Table 1: Maximum entrance air kerma rates for the 3 fluoroscopic modes I, II, and III on the reference and dose-reduction platforms^a

Platform, Mode	Frames/Second	Filtration	Maximum EAKR (mGy/min)
Reference			
I	6	0.4 mm Cu + 1 mm Al	22
II	12.5	0.4 mm Cu + 1 mm Al	44
III	12.5	0.1 mm Cu + 1 mm Al	79
DRT			
I	15	0.4 mm Cu + 1 mm Al	11
II	15	0.4 mm Cu + 1 mm Al	26
III	15	0.1 mm Cu + 1 mm Al	62

Note:—DRT indicates dose-reduction technology.

^a The operator chooses the fluoroscopy mode on the dose-reduction platform independent of the DSA program and the targeted dose-reduction setting used for angiography.

Table 2: Measured entrance air kerma rates for a typical patient examination and for the largest FOV in fluoroscopic mode II preferred for clinical imaging^a

System	DRT	Plane	kV	Focal Spot (mm)	Measured EAKR (mGy/min)	$\dot{K}_{a,r}$ Ratio
FD 20/20	No	AP	68 ± 1	Small (0.4)	5.1 ± 0.2	1.03 ± 0.12
		LAT	69 ± 1	Small (0.4)	6.1 ± 1.0	1.00 ± 0.04
FD 20/10	Before	AP	68 ± 1	Small (0.4)	4.9 ± 1.0	1.07 ± 0.03
		LAT	72 ± 4	Small (0.5)	6.3 ± 3.4	0.97 ± 0.004
	After	AP	68 ± 1	Small (0.4)	2.8 ± 0.4	0.96 ± 0.08
		LAT	73 ± 2	Small (0.5)	4.4 ± 0.6	1.01 ± 0.1

Note:—AP indicates anteroposterior; DRT, dose-reduction technology.

^a For each system, the selected kilovolt and x-ray focal spot along with its nominal size (millimeter) for each plane are summarized. For the FD 20/10 system, these values are reported before and after the installation of the DRT. The x-ray beam filtration is 0.4 mm Cu and 1 mm of Al for all systems, platforms, and planes.

Table 3: DSA programmed settings for the image-receptor (detector) entrance air kerma rate for a typical patient examination with the largest FOV on both platforms^a

System	DRT	Acquisition Protocol	kV	Filtration	Focal Spot (mm)	Programmed RAKR ($\mu\text{Gy}/\text{frame}$)
FD 20/20	No	Standard	80	0.1 mm Cu +1 mm Al	Large (AP/LAT: 0.7 mm)	4.0
FD 20/10	Before After	Standard	80	0.1 mm Cu +1 mm Al	Large (AP: 0.7 mm; LAT: 0.8 mm)	4.0
		Quarter	75	0.1 mm Cu +1 mm Al	Small (AP: 0.4 mm; LAT: 0.5 mm)	0.7
		Half	78	No added filtration	Small (AP: 0.4 mm; LAT: 0.5 mm)	1.0
		Full	80	0.1 mm Cu +1 mm Al	Large (AP: 0.7 mm; LAT: 0.8 mm)	4.0

Note:—AP indicates anteroposterior; DRT, dose-reduction technology.

^a The dose-reduction platform was equipped with 3 acquisition protocols in which the “full-dose” protocol reverts to the reference platform hardware and software settings (“standard” dose protocol). The programmed settings are identical for both planes in each system and for each acquisition protocol.

to system-reported data. Also, from Table 2, it can be inferred that for IP_{DRT} , the EAKR was approximately reduced by 50% compared with IP_{R} .

Regarding DSA acquisitions, the programmed settings for the image-receptor (detector) entrance air kerma rate (RAKR) for IP_{R} is shown in Table 3 and is referred to as “standard” acquisition protocol. The default setting programmed for the IP_{DRT} targeted an approximate 75% reduction in EAKR with respect to the IP_{R} , herein referred to as “quarter-dose” protocol. However, the neurointerventional radiologist, on the basis of patient-, procedure-, and acquisition-specific needs had the flexibility to select either the “quarter-dose” protocol; a “half-dose” protocol, which reduced the EAKR by approximately 50% with the dose-reduction technology; or, in rare circumstances, to revert to the reference platform hardware and software settings at 100% of the original dose, referred to as “full-dose” protocol and is identical to the “standard” protocol. The RAKRs for the 3 acquisition protocols are summarized in Table 3. The programmed settings were identical for both planes in each system and for each acquisition protocol.

Data Collection

The following information was retrospectively collected for each procedure or examination from the neurointerventional suites during the analyzed time period: procedure type classified into 10 categories (diagnostic angiography, aneurysm coil embolization, flow-diverter placement, intra-arterial vasospasm treatment, thrombectomy for acute ischemic stroke, stent-assisted aneurysm coiling, epistaxis treatment, carotid stent placement, brain AVM embolization, and dural AVF treatment), cumulative dose-area product in units of $\text{Gy} \times \text{cm}^2$, total fluoroscopy duration (minutes), administered contrast volume (milliliter), names of the neurointerventional radiologists performing the procedure or examination labeled as “operators,” and a selection of patient characteristics that may reflect differences in outcome measures. The collected patient characteristics included age, sex, body weight (kg), preprocedural blood pressure, and medical history such as hypertension, chronic obstructive pulmonary disorder, coronary artery disease, obesity, and diabetes mellitus. The patient characteristics were obtained from electronic medical records and procedure documents. Contrast volume was extracted from procedure documents. Cumulative dose (kerma)-area product and total fluoroscopy duration were extracted from procedure documents or retrieved from a Cloud-based dose-monitoring system (DoseWise Portal; Philips Healthcare). The dose-monitoring sys-

tem gathered and anonymized system-generated dose-area product (P_{KA}) for each fluoroscopic, angiographic, and 3D imaging acquisition, and the CP_{KA} was aggregated from all acquisitions for that procedure. The CP_{KA} reported in this study is for the entire procedure and is inclusive of 3D rotational angiography (3DRA) and conebeam CT (CBCT), if performed, which do not benefit from dose-reduction technology enabled by the IP_{DRT} platform.

Data Preparation

A total of 1592 procedures were performed during the 2-year period in the 2 suites. After excluding spinal procedures ($n = 260$), cases with multiple or mixed treatment procedures ($n = 11$), partial diagnostic or partial/follow-up treatment studies ($n = 14$), other non-neurointerventional procedures ($n = 25$), and aneurysm-embolization procedures without coils or flow diverters ($n = 4$), we included data for the remaining cases ($n = 1278$). Cases with ≥ 1 missing outcome variable ($n = 27$) or patient-related factors ($n = 13$) were discarded, resulting in 1238/1592 (77.7%) cases available for analysis.

The 3 outcome variables of interest analyzed in the study were CP_{KA} , fluoroscopy duration, and administered contrast volume. Four interventional neuroradiologists performed these procedures. For procedures involving >1 operator, we could not accurately apportion the outcome variables. Therefore, any procedure involving >1 operator was coded as >1 operator. Patient medical history, with the exception of hypertension, was binary-coded for each condition. History of hypertension was combined with the preprocedural blood pressure measurement to generate a 4-point categorical scale: 0, no history of hypertension with preprocedural systolic and diastolic measurements of <140 and 90 mm Hg, respectively; 1, a history of hypertension and preprocedural systolic and diastolic measurements of <140 and 90 mm Hg, respectively; 2, no history of hypertension and preprocedural systolic and diastolic measurements of either ≥ 140 or ≥ 90 mm Hg, respectively; and, 3, a history of hypertension and preprocedural systolic and diastolic measurements of either ≥ 140 or ≥ 90 mm Hg, respectively.

Statistical Analysis

All statistical analyses were performed by using SAS 9.3 (SAS Institute, Cary, North Carolina). Generalized linear models were used to quantify the changes in the 3 outcome measures between the 2 neurointerventional imaging platforms. The outcome variables were appropriately Box-Cox transformed before statistical modeling. All models included the platform type (IP_{DRT} or IP_{R})

and the neurointerventional procedure category as independent variables; and inclusion of covariates (operator, patient characteristics) was determined by using stepwise selection based on the corrected Akaike Information Criterion.¹⁵ For each model, the least squares means and the confidence intervals for each platform

and the Sidak multiple comparison–adjusted *P* values for the differences in least squares means between the 2 imaging platforms were obtained. The differences in least squares means between IP_{DRT} and IP_R and the percentage change were computed. Effects associated with *P* < .05 were considered statistically significant.

Table 4: Patient demographics and number of cases performed on each imaging platform^a

	Reference Platform	Dose-Reduction Platform
No. of cases		
Diagnostic	654 (71.6%)	173 (53.4%)
Coil embolization	45 (5.0%)	42 (12.2%)
Flow diverter	58 (6.5%)	26 (7.6%)
Vasospasm	34 (3.7%)	26 (8.0%)
Thrombectomy	37 (4.1%)	19 (5.5%)
Stent-assisted coiling	27 (3.0%)	15 (4.4%)
Carotid stenting	25 (2.8%)	9 (2.6%)
Epistaxis	17 (1.9%)	5 (1.5%)
AVM	10 (1.1%)	6 (1.7%)
AVF	7 (0.8%)	3 (0.9%)
Total	914 (73.8%)	324 (26.2%)
Patient characteristics		
Age (yr)	57.4 ± 14.7	56.6 ± 15.2
Weight (kg)	79.3 ± 19.9	77.6 ± 18.4
Male	370 (40.5%)	134 (41.4%)
Female	544 (59.5%)	190 (58.6%)
Hypertension	276 (30.2%)	89 (27.5%)
Medical history		
Diabetes	113 (12.4%)	39 (12.0%)
CAD	67 (7.3%)	21 (6.5%)
COPD	61 (6.7%)	26 (8.0%)
Hypertension	496 (54.3%)	177 (54.6%)
Obesity	53 (5.8%)	17 (5.2%)
Operator		
1	59 (6.5%)	18 (5.6%)
2	433 (47.4%)	175 (54.0%)
3	249 (27.2%)	23 (7.1%)
4	79 (8.6%)	92 (28.4%)
Multiple	94 (10.3%)	16 (4.9%)

Note:—CAD indicates coronary artery disease; COPD, chronic obstructive pulmonary disorder.

^a Data are presented as number (percentage) or mean ± SD. The number of patients with preprocedural hypertension is reported under “Patient characteristics,” while the number of patients with a documented history of hypertension is reported under “Medical history.”

Table 5: Reduction achieved with the dose-reduction platform in comparison with the reference platform^a

Procedure	CP _{KA} (Gy × cm ²)	Fluoroscopy Duration (min)	Contrast Volume (mL)
Diagnostic	88.2 (63.3%) ^b	−1.7 (−17.3%) ^c	−12.6 (−8.3%)
All interventions	171.8 (52.7%) ^b	−5.9 (−16.6)	−23.1 (−10.1%)
Coil embolization	166.3 (50.3%) ^b	−4.4 (−10.3%)	−37.3 (−13.7%)
Flow diverter	82.1 (30.5%) ^c	−14.9 (−55.1%) ^c	−34.6 (−15.5%)
Vasospasm	124.9 (71.1%) ^b	1.7 (11.1%)	9.4 (6.2%)
Thrombectomy	191.9 (60.2%) ^b	−5.1 (−17.8%)	2.9 (1.4%)
Stent-assisted coiling	112.1 (35.2%) ^c	−11.1 (−26.2%)	−72.6 (−27.1%) ^c
Carotid stenting	122.2 (55.7%) ^b	−1.7 (−6.7%)	17.6 (7.9%)
Epistaxis	251.0 (73.8%) ^b	−7.4 (−22.7%)	73.7 (30.2%)
AVM	165.4 (26.2%)	−8.9 (−8.7%)	−105.3 (−43.2%) ^c
AVF	222.4 (37.6%)	−24.9 (−36.2%)	−51.3 (−15.6%)
Overall	160.3 (53.2%) ^b	−5.2 (−16.8%) ^c	−15.3 (−6.7%)

^a Positive values indicate a reduction with the dose-reduction platform. Differences (percentage) in cumulative dose-area product, total fluoroscopy duration, and administered contrast volume were obtained from least squares means.

^b *P* < .0001.

^c *P* < .05.

RESULTS

Patient demographics and the number of cases are summarized in Table 4. Among the 1238 cases analyzed, 914 were performed on the IP_R and 324 were performed on the IP_{DRT}. The diagnostic examinations were 71.6% and 53.4% of the cases on the reference and dose-reduction platforms, respectively. All results are presented after adjusting for neurointerventional radiologist and patient characteristics in each model.

Procedural Cumulative Dose-Area Product

Overall and across all diagnostic examinations and neurointerventional procedures, the IP_{DRT} was associated with a significant reduction in procedural CP_{KA}, inclusive of all executed fluoroscopic, angiographic, and 3D imaging acquisitions (53.2%; mean reduction, 160.3 Gy × cm²; *P* < .0001) compared with the IP_R (Table 5). Most cases were diagnostic procedures (Table 4) and yielded a 63.3% reduction (mean reduction, 88.2 Gy × cm²; *P* < .0001) with IP_{DRT}. For diagnostic procedures, least squares means for the CP_{KA} were 139.4 Gy × cm² (95% CI, 131.6–147.6 Gy × cm²) for the IP_R and 51.1 Gy × cm² (95% CI, 47–55.6 Gy × cm²) for the IP_{DRT}. Across all interventional procedures, a 52.7% reduction (mean reduction, 171.8 Gy × cm²; *P* < .0001) was observed with IP_{DRT} compared with IP_R, and the least squares means for the CP_{KA} were 326.3 Gy × cm² (95% CI, 295.5–360.4 Gy × cm²) and 154.5 Gy × cm² (95% CI, 136–175.4 Gy × cm²) for IP_R and IP_{DRT}, respectively. The reduction in CP_{KA} ranged from 30.5% for flow-diverter implants (mean reduction, 82.1 Gy × cm²; *P* = .0015) to 73.8% for epistaxis (mean reduction, 251 Gy × cm²; *P* < .0001). Also, with the exception of dural AVFs (*n* = 7 and 3 for IP_{DRT} and IP_R, respectively) and brain AVMs (*n* = 10 and 6 for IP_{DRT} and IP_R, respectively), all procedure types showed a significant reduction in CP_{KA} with the IP_{DRT} (Table 5 and Fig 1).

Fluoroscopy Duration

Overall, the difference in total fluoroscopy duration between IP_{DRT} and IP_R was marginal (*P* = .0491) and resulted in a 5.2-minute (16.8%) increase with IP_{DRT} (Table 5 and Fig 2A). Procedure-related increases in fluoroscopy duration with the IP_{DRT} were found for diagnostic (an additional 1.7 minutes, *P* = .0002) and flow-diverter cases (an additional 14.9 minutes; *P* = .0038).

Administered Contrast Volume

Overall, the difference in administered contrast volume between IP_{DRT} and IP_R was nonsignificant (*P* = .1616) and resulted in a 15.3-mL (6.7%) increase with IP_{DRT} (Table 5 and Fig 2B). Increases in

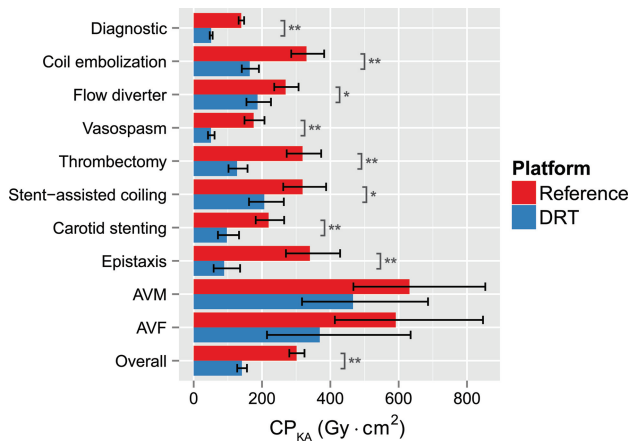


FIG 1. The cumulative dose-area product is significantly reduced with the dose-reduction technology platform. Bar graph and error bars represent least squares means and the associated 95% confidence intervals. Note a significant reduction in CP_{KA} between the dose-reduction technology and reference platforms. Asterisk indicates $P < .05$; double asterisks, $P < .0001$.

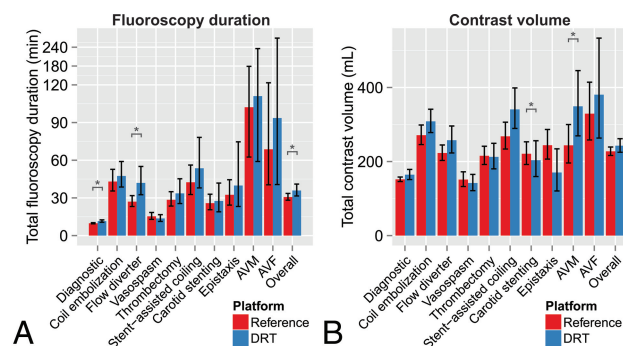


FIG 2. Least squares means and 95% confidence intervals of total fluoroscopy duration (A) and total administered contrast volume (B) are plotted for the reference and dose-reduction technology platforms. Note significant differences in fluoroscopy duration or contrast volume between the dose-reduction technology and reference platforms. Asterisk indicates $P < .05$; double asterisks, $P < .0001$.

administered contrast volume with the IP_{DRT} were observed for brain AVMs and stent-assisted coiling (Table 5 and Fig 2B).

DISCUSSION

While serious deterministic eye and skin injuries including cataracts are rare, erythema, and epilation as a consequence of interventional procedures are likely in a very small percentage of patients.^{16,17} Several joint-society initiatives have been launched in response to increased recognition of the need to address such deterministic and long-term stochastic adverse events by carefully considering radiation exposure across medical imaging procedures, particularly in pediatric populations. The Image Wisely campaign was unveiled by the Joint Task Force on Adult Radiation Protection, an initiative established in 2009 by the American College of Radiology and the Radiological Society of North America.¹⁸ Around the same time, the Alliance for Radiation in Pediatric Imaging introduced the Image Gently, Step Lightly campaign to encourage dose reduction in pediatric interventional radiologic procedures.¹⁹

General effort to minimize the risk of skin injury during fluoro-

scopic procedures entails using proper applied x-ray tube potential and beam filtration, limiting exposure duration for fluoroscopy, DSA, and non-DSA digital acquisitions, modifying the x-ray beam geometry by appropriate collimation and by placing the imaging detector close to the patient, and by ensuring minimal biplane overlap.²⁰ Besides educating interventional practitioners and technical staff on As Low As Reasonably Achievable practices, improvement in angiographic systems technology is needed to achieve further dose reductions while maintaining acceptable image quality.

The introduction of the IP_{DRT} with flexible selection of dose-reduction protocols to suit clinical needs was associated with an overall reduction in CP_{KA} of 53.2% across all diagnostic and interventional procedures in our academic neurointerventional practice. For diagnostic examinations, which constituted the largest fraction of studies, the mean CP_{KA} of $139.4 \text{ Gy} \times \text{cm}^2$ (95% CI, $131.6\text{--}147.6 \text{ Gy} \times \text{cm}^2$) observed in this study for the IP_R is lower than the $162.2 \pm 231.7 \text{ Gy} \times \text{cm}^2$ (95% CI, $129.0\text{--}195.4 \text{ Gy} \times \text{cm}^2$) reported by Söderman et al.⁵ In this study, the flexible use of dose-reduction protocols with the default setting of a quarter-dose protocol for the IP_{DRT} reduced the cumulative dose (kerma)-area product to $51.1 \text{ Gy} \times \text{cm}^2$ (95% CI, $47\text{--}55.6 \text{ Gy} \times \text{cm}^2$) constituting a 63.3% reduction with respect to the IP_R , similar to the 62% reduction in CP_{KA} with the fixed quarter-dose protocol reported by Söderman et al. Fig 3 shows a sample case highlighting improved visualization of perforators in diagnostic angiography with the half-dose and quarter-dose protocols.

Previous surveys of dose reports from a variety of interventional practices were used to infer reference dose values.^{21–24} In addition, estimates of radiation doses for smaller groups of patients and for various neurointerventional procedures have been reported.^{25–27} For the reference platform (IP_R), our CP_{KA} estimate of $139.4 \text{ Gy} \times \text{cm}^2$ (95% CI, $131.6\text{--}147.6 \text{ Gy} \times \text{cm}^2$) for diagnostic procedures is consistent with earlier reports by Kien et al.²³ ($173.9 \pm 90.9 \text{ Gy} \times \text{cm}^2$), D'Ercole et al.²⁴ ($142.1 \pm 75.5 \text{ Gy} \times \text{cm}^2$), Söderman et al.⁵ ($162.2 \pm 231.7 \text{ Gy} \times \text{cm}^2$; 95% CI, $129.0\text{--}195.4 \text{ Gy} \times \text{cm}^2$), and Alexander et al.²⁵ ($102.4 \pm 43.4 \text{ Gy} \times \text{cm}^2$). In addition, for aneurysm coil embolization, our CP_{KA} estimates of $330.3 \text{ Gy} \times \text{cm}^2$ (95% CI, $285.6\text{--}381.9 \text{ Gy} \times \text{cm}^2$) for IP_R are not markedly different from those reported by Miller et al.²¹ ($282.7 \text{ Gy} \times \text{cm}^2$; 95% CI, $261.1\text{--}304.3 \text{ Gy} \times \text{cm}^2$), D'Ercole et al.²⁸ ($413 \text{ Gy} \times \text{cm}^2$; 95% CI, $343\text{--}482 \text{ Gy} \times \text{cm}^2$), Kien et al.²³ ($275.7 \pm 145.1 \text{ Gy} \times \text{cm}^2$), D'Ercole et al.²⁴ ($369.5 \pm 162.3 \text{ Gy} \times \text{cm}^2$), Vano et al.²⁷ ($293 \pm 188 \text{ Gy} \times \text{cm}^2$ and $317 \pm 234 \text{ Gy} \times \text{cm}^2$), and Alexander et al.²⁵ ($172.3 \pm 67.7 \text{ Gy} \times \text{cm}^2$).

The wide range of CP_{KA} reported in this and prior studies reflects the diverse nature of neurointerventional procedures performed with varying degrees of complexity, partly due to the expanded repository of neurointerventional devices such as Onyx (Covidien, Irvine, California), which is known to increase the procedure duration for AVM embolization,²⁹ and to the enhanced capabilities of the imaging equipment, such as the ability to perform 3DRA and CBCT. The procedural CP_{KA} reported in this study is inclusive of 3DRA and CBCT. Hence, caution is warranted while comparing results from this study with those of earlier studies, in which such 3D acquisitions were not prevalent, different devices were used, and case complexity

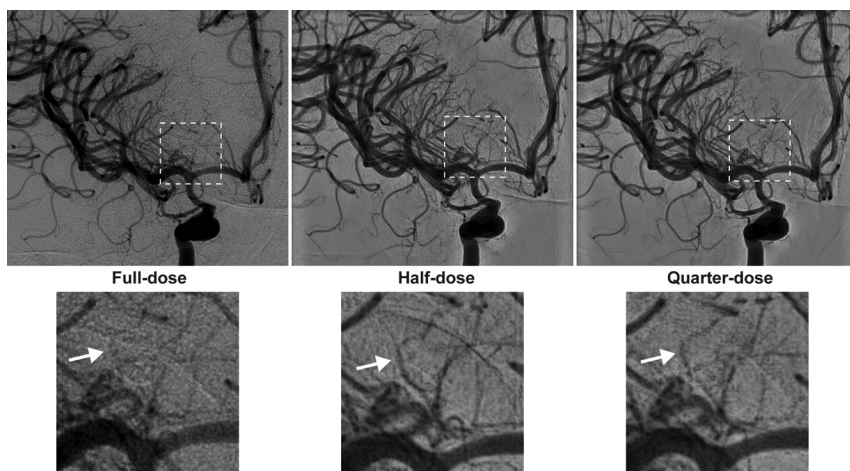


FIG 3. Diagnostic angiography was performed to assess the source of bleeding in a 43-year-old man who presented with diffuse SAH. During the examination, angiograms after contrast administration into the right ICA were obtained on IP_{DRT} platform by using the “full-dose” protocol (left), which is identical to the reference platform in terms of hardware and software settings, “half-dose” protocol (middle), and “quarter-dose” protocol (right). Magnified views of the dashed area highlight improved visualization of small perforators (white arrows) with the “half-dose” and “quarter-dose” protocols (lower panels).

was difficult to assess. The advantage of our analysis for comparison of IP_{DRT} and IP_R is that it is adjusted for operator and patient characteristics under identical practice standards with independent confirmation of system-reported CP_{KA}.

For the IP_{DRT}, the dose-reduction technology and the reduced air kerma rates are active only during 2D acquisitions such as fluoroscopy and DSA. For procedures requiring CBCT scans and depending on the number and type of CBCT scans, the relative benefit of the IP_{DRT} in terms of cumulative dose (kerma)-area product is reduced. For instance, flow-diverter placement at our institution commonly requires 3DRA before device deployment and at least 2 CBCT image volumes following implantation to confirm proper deployment and the absence of intraprocedural hemorrhage. Moreover, because flow-diverter placement is generally accompanied only by several angiograms before and after device deployment, the opportunities for dose reduction are relatively limited. For flow-diverter placement, the mean CP_{KA} for the IP_R and IP_{DRT} was 269.1 and 187 Gy × cm², respectively, constituting a significant ($P = .0015$) but relatively modest 30.5% reduction. Even in aneurysm coil embolization, an initial 3DRA and final CBCT are performed as standard of practice at our institution. Analysis of a subset of cases in which P_{KA} measurements were available separately for fluoroscopy, DSA, and CBCT suggests that there was no difference in the relative contribution of CBCT to the procedural CP_{KA} between the IP_R and IP_{DRT} for diagnostic cases, while results acquired on the IP_{DRT} indicate that the relative contribution of the CBCT to the CP_{KA} may vary with procedure type (On-line Figs 1 and 2 and On-line Table).

The study observed CP_{KA} reduction with the IP_{DRT} for each procedure type, with the exception of dural AVFs and brain AVMs. On occasion, an operator may repeat an acquisition at a higher dose for verification. However, in practice these situations arose sporadically, such as when examining highly complex brain AVMs, and rarely occurred during most of the diagnostic and other treatment proce-

dures. The limited sample size for brain AVMs (10 and 6 treated on the IP_R and IP_{DRT}, respectively) and dural AVFs (7 and 3 treated on the IP_R and IP_{DRT}, respectively) could have also contributed to a nonsignificant reduction ($P > .15$) to the procedure CP_{KA}.

Despite significant reductions in CP_{KA} and across most procedure types, overall, we observed a marginal difference ($P = .0491$) in total fluoroscopy duration between the 2 platforms, with an additional 5.2 minutes of fluoroscopy duration with the IP_{DRT}. On our systems, the default is fluoroscopy mode II and is typically used for interventions. Generally, fluoroscopy mode I was used for diagnostic examinations, and fluoroscopy mode III was reserved for complex cases involving flow-diverter placement and AVM embolization. There was no indication

that the use of these modes was different between the IP_R and the IP_{DRT}. Significant differences in total fluoroscopy duration between the 2 platforms were observed for diagnostic examinations ($P = .0002$) and flow-diverter placement ($P = .0038$), with an increase of 1.7 and 14.9 minutes, respectively, with IP_{DRT}. Additional analyses for these procedures indicated that the total fluoroscopy duration with IP_{DRT} increased for 1 operator by 2.3 minutes for diagnostic examinations ($P < .0001$) and 10.7 minutes for flow-diverter placement ($P = .0026$). Also, for flow-diverter placement, procedures involving >1 operator contributed to a substantial 34.5-minute ($P = .0203$) increase with IP_{DRT}. In our academic practice, the extent to which the assisting fellows are involved and the nature of their contribution to a case, depending on the procedure, may vary. Regarding the total administered contrast volume, overall, the difference between the 2 platforms was nonsignificant ($P = .1616$), with an increase of 15.3 mL (6.7%) with IP_{DRT}. Overall, the marginal increase in fluoroscopy duration and the nonsignificant change in administered contrast volume suggest that workflow was unaffected by the use of the IP_{DRT}.

Our study had limitations. This retrospective study precluded randomization of the operator and imaging platform. We did not analyze the partial contributions to CP_{KA} from fluoroscopy, angiography, and 3D imaging for all cases because these data were not recorded uniformly. For each procedure type, the sample-size distribution was not uniform for the 2 platforms in this retrospective study. Another confounding factor is the smaller x-ray detector for the LAT plane of the FD20/10 system, which was used for all IP_{DRT} examinations and part of the IP_R examinations. The smaller detector size may contribute to lower P_{KA} for that acquisition or may contribute to higher procedural CP_{KA}, because adjacent regions were additionally imaged when clinically needed. At our institution, all neurointerventional systems are from a single vendor; hence, our analysis is restricted to that vendor. Our study

considered CP_{KA} alone as the metric for analysis and does not address the skin-dose distribution and the peak skin dose³⁰ because the imaging geometry relative to the patient and anatomic region was not collected. CP_{KA} is relevant to the estimation of stochastic effects, while peak skin dose is directly related to skin effects.

CONCLUSIONS

The introduction of a dose-reduction platform was associated with a significant reduction of 53.2% in CP_{KA} over all procedure types, ranging from 30.5% to 73.8% for individual procedures compared with the reference platform without the noise-reduction algorithm from the same vendor. After adjustment for the operating neurointerventional radiologist and patient characteristics, our results demonstrate that significant dose reductions can be achieved for almost all the considered procedure types. Only marginal effects on total fluoroscopy duration and total administered contrast volume were observed, suggesting that the impact on workflow was minimal.

Disclosures: Imrasmah M.J. van der Bom—UNRELATED: Employment: Philips Healthcare; Stock/Stock Options: InNeuroCo. Matthew J. Gounis—RELATED: Grant: Philips Healthcare*; UNRELATED: Consultancy: Codman Neurovascular, Stryker Neurovascular; Grants/Grants Pending: National Institutes of Health, Asahi Intecc, Blockade Medical, CereVasc LLC, Codman Neurovascular, Cook Medical, Gentuity LLC, Fraunhofer Institute, InNeuroCo, Lazarus Effect, Medtronic, MicroVention/Terumo, Philips Healthcare, Silk Road, Spineology, Stryker Neurovascular, Wyss Institute*; Stock/Stock Options: InNeuroCo. Ajit S. Puri—UNRELATED: Consultancy: Stryker Neurovascular, Codman Neurovascular; Grants/Grants Pending: Stryker Neurovascular, Covidien*; Stock/Stock Options: InNeuroCo; Travel/Accommodations/Meeting Expenses Unrelated to Activities Listed: Stryker Neurovascular. Ajay K. Wakhloo—RELATED: Grant: Philips Healthcare, Comments: equipment support and research grant*; Support for Travel to Meetings for the Study or other Purposes: Philips Healthcare*; UNRELATED: Consultancy: Codman Neurovascular, Stryker Neurovascular; Expert Testimony: McCoy Law Firm, Coral Gables, Florida; Payment for Lectures, including Service on Speakers Bureaus: Harvard postgraduate course, Miami Cardiac and Vascular Institute; Stock/Stock Options: InNeuroCo, EpiEP, Penumbra; Other: Pulsar Medical, Comments: bridge loan. *Money paid to the institution.

REFERENCES

- Molyneux AJ, Kerr RS, Yu LM, et al; International Subarachnoid Aneurysm Trial (ISAT) Collaborative Group. **International subarachnoid aneurysm trial (ISAT) of neurosurgical clipping versus endovascular coiling in 1413 patients with ruptured intracranial aneurysms: a randomised comparison of effects on survival, dependency, seizures, rebleeding, subgroups, and aneurysm occlusion.** *Lancet* 2005;366:809–17 [CrossRef Medline](#)
- Grigoryan M, Chaudhry SA, Hassan AE, et al. **Neurointerventional procedural volume per hospital in United States: implications for comprehensive stroke center designation.** *Stroke* 2012;43:1309–14 [CrossRef Medline](#)
- Stecker MS, Balter S, Towbin RB, et al; SIR Safety and Health Committee; CIRSE Standards of Practice Committee. **Guidelines for patient radiation dose management.** *J Vasc Interv Radiol* 2009;20(suppl):S263–73 [CrossRef Medline](#)
- Sánchez RM, Vano E, Fernández JM, et al. **Staff doses in interventional radiology: a national survey.** *J Vasc Interv Radiol* 2012;23:1496–501 [CrossRef Medline](#)
- Söderman M, Mauti M, Boon S, et al. **Radiation dose in neuroangiography using image noise reduction technology: a population study based on 614 patients.** *Neuroradiology* 2013;55:1365–72 [CrossRef Medline](#)
- Pitton MB, Kloeckner R, Schneider J, et al. **Radiation exposure in vascular angiographic procedures.** *J Vasc Interv Radiol* 2012;23:1487–95 [CrossRef Medline](#)
- Söderman M, Holmin S, Andersson T, et al. **Image noise reduction algorithm for digital subtraction angiography: clinical results.** *Radiology* 2013;269:553–60 [CrossRef Medline](#)
- Nakamura S, Kobayashi T, Funatsu A, et al. **Patient radiation dose reduction using an X-ray imaging noise reduction technology for cardiac angiography and intervention.** *Heart Vessels* 2016;31:655–63 [CrossRef Medline](#)
- van Strijen MJ, Grünhagen T, Mauti M, et al. **Evaluation of a noise reduction imaging technology in iliac digital subtraction angiography: noninferior clinical image quality with lower patient and scatter dose.** *J Vasc Interv Radiol* 2015;26:642–50.e1 [CrossRef Medline](#)
- van den Haak RF, Hamans BC, Zuurmond K, et al. **Significant radiation dose reduction in the hybrid operating room using a novel x-ray imaging technology.** *Eur J Vasc Endovasc Surg* 2015;50:480–86 [CrossRef Medline](#)
- Ten Cate T, van Wely M, Gehlmann H, et al. **Novel X-ray image noise reduction technology reduces patient radiation dose while maintaining image quality in coronary angiography.** *Neth Heart J* 2015;23:525–30 [CrossRef Medline](#)
- Eloot L, Thierens H, Taeymans Y, et al. **Novel X-ray imaging technology enables significant patient dose reduction in interventional cardiology while maintaining diagnostic image quality.** *Catheter Cardiovasc Interv* 2015;86:E205–12 [CrossRef Medline](#)
- Haas NA, Happel CM, Mauti M, et al. **Substantial radiation reduction in pediatric and adult congenital heart disease interventions with a novel X-ray imaging technology.** *IJC Heart & Vasculture* 2015;6:101–09 [CrossRef](#)
- Lin PJ, Schueler BA, Balter S, et al. **Accuracy and calibration of integrated radiation output indicators in diagnostic radiology: a report of the AAPM Imaging Physics Committee Task Group 190.** *Med Phys* 2015;42:6815–29 [CrossRef Medline](#)
- Hurvich CM, Tsai CL. **Regression and time-series model selection in small samples.** *Biometrika* 1989;76:297–307 [CrossRef](#)
- Balter S, Hopewell JW, Miller DL, et al. **Fluoroscopically guided interventional procedures: a review of radiation effects on patients' skin and hair.** *Radiology* 2010;254:326–41 [CrossRef Medline](#)
- Faulkner K, Vañó E. **Deterministic effects in interventional radiology.** *Radiat Prot Dosimetry* 2001;94:95–98 [CrossRef Medline](#)
- Brink JA, Amis ES Jr. **Image Wisely: a campaign to increase awareness about adult radiation protection.** *Radiology* 2010;257:601–02 [CrossRef Medline](#)
- Sidhu M, Goske MJ, Connolly B, et al. **Image Gently, Step Lightly: promoting radiation safety in pediatric interventional radiology.** *AJR Am J Roentgenol* 2010;195:W299–301 [CrossRef Medline](#)
- Norbash AM, Busick D, Marks MP. **Techniques for reducing interventional neuroradiologic skin dose: tube position rotation and supplemental beam filtration.** *AJNR Am J Neuroradiol* 1996;17:41–49 [Medline](#)
- Miller DL, Balter S, Cole PE, et al; RAD-IR study. **Radiation doses in interventional radiology procedures: the RAD-IR study, part I: overall measures of dose.** *J Vasc Interv Radiol* 2003;14:711–27 [CrossRef Medline](#)
- Vano E, Järvinen H, Kosunen A, et al. **Patient dose in interventional radiology: a European survey.** *Radiat Prot Dosimetry* 2008;129:39–45 [CrossRef Medline](#)
- Kien N, Rehel JL, Etard C, et al. **Patient dose during interventional neuroradiology procedures: results from a multi-center study [in French].** *J Radiol* 2011;92:1101–12 [CrossRef Medline](#)
- D'Ercole L, Thyron FZ, Bocchiola M, et al. **Proposed local diagnostic reference levels in angiography and interventional neuroradiology and a preliminary analysis according to the complexity of the procedures.** *Phys Med* 2012;28:61–70 [CrossRef Medline](#)
- Alexander MD, Oliff MC, Olorunsola OG, et al. **Patient radiation exposure during diagnostic and therapeutic interventional neuro-radiology procedures.** *J Neurointerv Surg* 2010;2:6–10 [CrossRef Medline](#)
- Chohan MO, Sandoval D, Buchan A, et al. **Cranial radiation exposure during cerebral catheter angiography.** *J Neurointerv Surg* 2014;6:633–36 [CrossRef Medline](#)

27. Vano E, Fernandez JM, Sanchez RM, et al. **Patient radiation dose management in the follow-up of potential skin injuries in neuroradiology.** *AJNR Am J Neuroradiol* 2013;34:277–82 [CrossRef](#) [Medline](#)
28. D’Ercole L, Mantovani L, Thyryon FZ, et al. **A study on maximum skin dose in cerebral embolization procedures.** *AJNR Am J Neuroradiol* 2007;28:503–07 [Medline](#)
29. Velat GJ, Reavey-Cantwell JF, Sistrom C, et al. **Comparison of N-butyl cyanoacrylate and Onyx for the embolization of intracranial arteriovenous malformations: analysis of fluoroscopy and procedure times.** *Neurosurgery* 2008;63:ONS73–78; discussion ONS78–80 [Medline](#)
30. Khodadadegan Y, Zhang M, Pavlicek W, et al. **Validation and initial clinical use of automatic peak skin dose localization with fluoroscopic and interventional procedures.** *Radiology* 2013;266:246–55 [CrossRef](#) [Medline](#)